

Article

Metabolite Profiling Analysis of the Tongmai Sini Decoction in Rats after Oral Administration through UHPLC-Q-Exactive-MS/MS

Xianhui Zheng ^{1,2}, Yingying Zhan ¹, Mengling Peng ¹, Wen Xu ^{1,2} and Guanghai Deng ^{1,2,*}

¹ The Second Clinical College, Guangzhou University of Chinese Medicine, Guangzhou 510006, China; xianhui Zheng@gzucm.edu.cn (X.Z.); 20221110784@stu.gzucm.edu.cn (Y.Z.); 20221110783@stu.gzucm.edu.cn (M.P.); fantasy@gzucm.edu.cn (W.X.)

² Guangdong Provincial Hospital of Chinese Medicine, Guangzhou 510120, China

* Correspondence: guanghai.deng@gzucm.edu.cn

Abstract: Tongmai Sini decoction (TSD), the classical prescriptions of traditional Chinese medicine, consisting of three commonly used herbal medicines, has been widely applied for the treatment of myocardial infarction and heart failure. However, the absorbed components and their metabolism in vivo of TSD still remain unknown. In this study, a reliable and effective method using ultra-performance liquid chromatography coupled with hybrid quadrupole-Orbitrap mass spectrometry (UHPLC-Q-Exactive-MS/MS) was employed to identify prototype components and metabolites in vivo (rat plasma and urine). Combined with mass defect filtering (MDF), dynamic background subtraction (DBS), and neutral loss filtering (NLF) data-mining tools, a total of thirty-two major compounds were selected and investigated for their metabolism in vivo. As a result, a total of 82 prototype compounds were identified or tentatively characterized in vivo, including 41 alkaloids, 35 phenolic compounds, 6 saponins. Meanwhile, a total of 65 metabolites (40 alkaloids and 25 phenolic compounds) were tentatively identified. The metabolic reactions were mainly hydrogenation, demethylation, hydroxylation, hydration, methylation, deoxygenation, and sulfation. These findings will be beneficial for an in-depth understanding of the pharmacological mechanism and pharmacodynamic substance basis of TSD.

Keywords: Tongmai Sini decoction; metabolites profiles; metabolic pathways; UHPLC-Q-Exactive-MS/MS



Citation: Zheng, X.; Zhan, Y.; Peng, M.; Xu, W.; Deng, G. Metabolite Profiling Analysis of the Tongmai Sini Decoction in Rats after Oral Administration through UHPLC-Q-Exactive-MS/MS. *Metabolites* **2024**, *14*, 333. <https://doi.org/10.3390/metabo14060333>

Academic Editors: Hirokazu Kawagishi and Junsong Wang

Received: 23 April 2024

Revised: 28 May 2024

Accepted: 3 June 2024

Published: 14 June 2024



Copyright: © 2024 by the authors. Licensee MDPI, Basel, Switzerland. This article is an open access article distributed under the terms and conditions of the Creative Commons Attribution (CC BY) license (<https://creativecommons.org/licenses/by/4.0/>).

1. Introduction

The classical prescriptions of traditional Chinese medicine (TCM) have originated from the fixed combination of certain kinds of herbal medicines recorded in the ancient classics, which have been still widely used in East Asia and exhibited precise clinical efficacy, with obvious characteristics and advantages [1]. For a long time, some classic prescriptions have been developed into modern Chinese medicinal preparations through the optimization of preparation technology and drug development research [2,3]. Most classical prescriptions have existed for at least hundreds of years, and with time, classic prescriptions may have changed to some extent, while their core characteristics (e.g., composition of herbs, proportion of herbs, etc.) have not changed significantly [4,5]. The reasons for the inheritance of classical prescriptions to the present day can be attributed to the high safety of the prescriptions and their proven efficacy due to a large number of clinical applications.

Tongmai Sini decoction (TSD) is a classic formula from the Chinese medical masterpiece “The Treatise on Typhoid Fever”, written 1800 years ago. It consists of three herbal concoctions of *Radix Aconiti Lateralis Preparata* (RALP), *Rhizoma Zingiberis* (RZ), and *Radix Glycyrrhizae Preparata* (RGP) and is commonly used in modern times for myocardial infarction and heart failure, atherosclerosis, shock, diarrhea, etc. [6,7]. TSD has the effects of

raising blood pressure, strengthening the heart, anti-hypoxia, anti-shock, anti-thrombosis, anti-myocardial ischemia, anti-slowng arrhythmia, and so on [8,9]. The main chemical constituents of TSD include alkaloids (from RALP), phenolic acids and saponins (from RGP), and volatile oils (from RZ). At present, chemical composition [10], pharmacological, pharmacokinetic [11–13], and metabolomics [8,9,14] studies have been preliminarily conducted on TSD, especially on its cardiovascular activities. Most of the studies on TDS concentrated on the pharmacokinetics of diterpene alkaloids after oral administration of TDS, and some of the studies focused on the changes in the in vivo metabolome or lipidome profile against myocardial ischemia, heart failure, hypothyroidism. There is a lack of systematic and in-depth in vivo chemical and metabolite studies of TDS.

The components of different botanicals enter the body and produce metabolites, which exert therapeutic effects through multiple pathways [15]. To fully understand the therapeutic components, it is necessary to first analyze the blood-entering components and their metabolites, as well as to study the metabolites distributed in plasma, urine, feces, and tissues, which is conducive to analysis of the potential components and pathways of action in the body [16,17].

High-resolution mass spectrometry (HRMS), in combination with chromatography technology, has provided useful structural information about chemical components, offering strong support for the characterization of in vivo and in vitro metabolic components of botanicals [18–20]. In recent years, in order to improve the sensitivity and selectivity of obtaining MS/MS or MSⁿ data for trace components in vivo, some acquisition and identification strategies have been developed, combined, and applied, for instance, the extracted ion chromatogram (EIC), mass defect filter (MDF), dynamic background subtraction (DBS) and neutral loss filter (NLF) [21–23].

In this paper, the established UHPLC-Q-Exactive-MS/MS methods have great advantages for the qualitative analysis of bioactive samples in rats after oral doses of TSD, and a variety of post-data processing techniques, including EIC, MDF, DBS, and NLF was applied for quickly screen and systematically identify the metabolites. These metabolic studies can provide the chemical foundation and an in-depth understanding of metabolic transformation for further research on effective substances and the action mechanism of TSD.

2. Materials and Methods

2.1. Chemicals and Plant Materials

Aconitine, mesaconitine, hyaconitine, liquiritin, liquiritigenin, ononin, and formononetin, with purities greater than 98%, were purchased from Shanghai Yuanye Biological Technology Co., Ltd. (Shanghai, China). HPLC-grade acetonitrile, methanol, and formic acid were purchased from Sigma Aldrich (St. Louis, MO, USA). Ultrapure Water (18.2 MΩ) was produced by a Milli-Q water system (Millipore, Bedford, MA, USA). The herbal pieces of RALP, RZ, and RGP were purchased from Kangmei Pharmaceutical Co. Ltd. Of Guangdong, China, and identified by Prof. Zhi-hai Huang, The Second Clinical College, Guangzhou University of Chinese Medicine, Guangzhou, China.

2.2. Plant Extract Preparation

According to the documentary records of TSD, the TSD pieces that included RALP (30 g), RZ (20 g), and RGP (30 g) were soaked with 8 times the amount of water for 30 min and decocted to boil (100 °C) for 2 h. The filtrate was collected, and the residue was decocted in 8 times the amount of water for 1.5 h again. The hot filtrate was combined and concentrated to 80 mL (1 g herbal pieces/1 mL aqueous solution). The obtained TSD extract was stored at –20 °C before use.

2.3. Animal and Drug Administration

Male Sprague–Dawley rats (220–260 g) were obtained from Guangdong Provincial Medical Laboratory Animal Center (Guangdong, China). All animal experiments were performed at the SPF animal laboratory [experimental animals license number SYXK

(Guangdong, China) 2008–0094]. The Institutional Animal Ethics Committee of Guangdong Provincial Hospital of Chinese Medicine approved all experimental protocols (No. 2023131).

Six SD rats were randomly divided into two groups (Urine and plasma groups) and adapted to the metabolic cage for a week before the experiment. Blank urine and plasma samples were collected under abrosia state ahead of gastric gavage. The rats were fasted for 14 h with water ad libitum before oral administration of TSD extract and underwent 4 h of water deprivation after that. TSD extract was orally administered to rats of urine and plasma groups twice at an interval of 1 h, and the dosage was 2 mL per 100 g bodyweight per time.

2.4. Sample Collection and Pretreatment

Urine samples from 0 to 24 h after the second dosing were collected and stored at $-80\text{ }^{\circ}\text{C}$ prior to analysis. Plasma samples were obtained at 1, 2, 4, 8, and 12 h after the second administration in heparinized 1.5 mL polythene tubes under diethyl ether anesthesia, respectively. All plasma samples were centrifuged at 4000 rpm for 10 min, and the plasma supernatants were then merged in equal volume and frozen at $-80\text{ }^{\circ}\text{C}$ prior to analysis.

The collected urine and plasma samples (200 μL) were added with $4\times$ the volume of acetonitrile-methanol (3:1) to precipitate protein, respectively. All separate supernatants were dried under N_2 flow, and the residues were resuspended in 200 μL acetonitrile and centrifuged at $15,000\times g$ for 8 min. Finally, a 5 μL sample was injected into the UHPLC-Q-Exactive-Orbitrap MS system for further analysis.

2.5. Instrumentation and Conditions

LC analyses were conducted on a Thermo UltiMate 3000 UHPLC system (Thermo Fisher Scientific, San Jose, CA, USA) equipped with a quaternary pump, a cooling autosampler, and a thermostatically controlled column oven. An ACQUITY UPLC HSS T3 Column (2.1 \times 100 mm, 1.8 μm) was used. The mobile solvents were composed of acetonitrile (A) and water with 0.02% formic acid (B), and the gradient elution profile was employed as follows: 5% A, 0 min; 16% A, 12 min; 55% A, 23 min; 90% A, 35 min; 95% A, 40 min; returning to initial conditions in 4 min at a flow rate of 200 $\mu\text{L}/\text{min}$ at room temperature. The injection volume was 5 μL . The temperatures of the sample tray and the column oven were set at 4 and 35 $^{\circ}\text{C}$, respectively.

A Q-Exactive hybrid quadrupole-orbitrap mass spectrometer was connected to an LC system via an electrospray ionization source as an interface. Data acquisition and processing were calculated using Compound Discoverer 3.2 software. The optimized parameters for MS analysis were as follows: the mass spectrometer parameters were positive (PI) and negative (NI) ion mode; the resolution of the Orbitrap mass analyzer was set as 30,000; ion spray voltage was -3.8 kV ; the capillary temperature was 325 $^{\circ}\text{C}$; the sheath gas flow rate was 40 psi; the auxiliary gas flow rate was 8 psi; and the mass range was m/z 150–1500. The properties of data-dependent MS^2 scanning (DDS) parameters and events were as follows: resolution, 17,500; HCD, 35 eV; repeat count, 2; exclusion list, 50; repeat duration, 5 s; and exclusion duration, 30 s. The mass error for molecular ions of all compounds identified was within ± 5 ppm.

3. Results and Discussion

3.1. Systematic Analytical Strategy for Online Metabolite Analysis

Based on our previous research on the cleavage patterns of components in RALP and RGP and a review of the literature [24–28], the metabolite profiling of TSD was systematically investigated by UHPLC-Q-Exactive-MS/MS methods. The workflow of the analytic procedure was carried out and shown in Figure 1. Figures S1 and S2 (Supplementary Materials) displayed the detailed workflow for the identification of prototype components and metabolites, respectively.

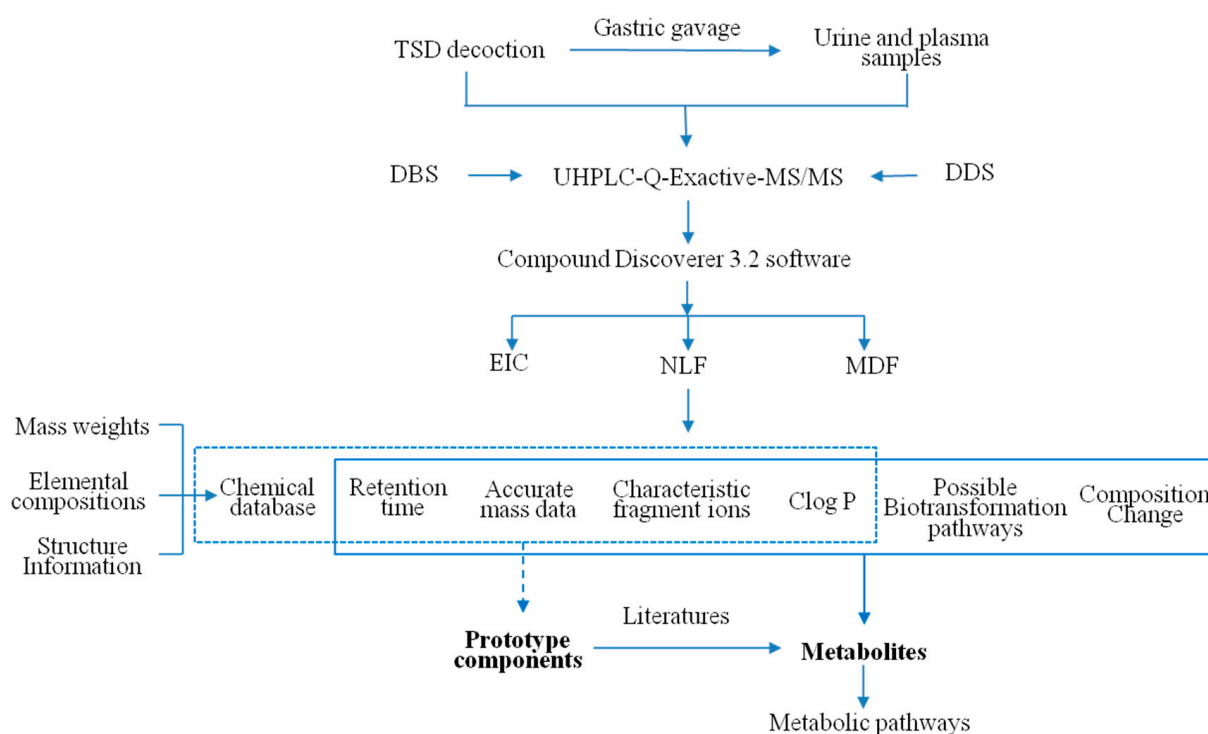


Figure 1. Workflow of the analytic strategy for the metabolite identification of TSD.

The strategy consisted of the following steps: (1) First, the chemical database (Table S1, Supplementary Materials) was constructed, including mass weights, elemental compositions, and structure information of chemical compositions originating from RALP, RGP, and RZ based on our previous research and the related literature [24–29]. (2) Then, an online full-scan and MS/MS data acquisition was processed in both negative and positive modes based on the DBS and DDS techniques for potential metabolite detection. (3) Next, the data files were imported into the Compound Discoverer 3.2 software, and the data-mining tools of EIC, NLF, and MDF were applied to screen the possible metabolites of TSD. Table S2 (Supplementary Materials) showed the detailed parameters of data processing. The main compounds with mass spectral peak areas greater than 10^8 in the decoction (shown in Table 1) were used as parent compound templates for MDF data screening (± 50 mDa) (4) Next, based on the chemical database, acquired accurate mass data, retention time, and characteristic fragment ions, the identification of prototype components was elucidated (shown in Table 2). In addition, the $\text{Clog } p$ values calculated by ChemDraw 14.0 were used to distinguish isomers at different retention times. (5) Finally, the mass information of potential metabolites, as well as their possible biotransformation pathways and composition change given by Compound Discoverer 3.2, were compared by the data of prototype components and the related literature to verify the metabolites and their metabolic pathways (shown in Table 3).

Table 1. Main prototype components as parent compound templates for MDF data screening. (mass spectral peak areas greater than 10^8 in the decoction).

Alkaloids (from RALP)	Phenolic and Saponin Compounds (from RGP and RZ)	
Karakolidine	Liquiritigenin	Formononetin
Fuziline	Isoliquiritigenin	Ononin
Neoline	Liquiritin	Glycyrrhizic Acid
Songorine	Licochalcone B	Glycyrrhetic Acid
14-Benzoylhypaconine	Licochalcone C	Uralsaponin C
Talatizamine	Licochalcone D	Licoricesaponin G2
Karakoline	Licoflavone C	Glycycoum-Arim

Table 1. Cont.

Alkaloids (from RALP)	Phenolic and Saponin Compounds (from RGP and RZ)	
14-Benzoylmesaconine	Licoflavone A	Glycyrol
Mesaconitine	Licoricidin	Glycyrin
Hypaconitine	Licoleafol	6-Gingerol
Aconitine	Gancaonin M	

3.2. Identification of Prototype Components

An in-house database has been established for each compound involved in RALP, RGP, and RZ based on our previous experimental data and the related literature for the investigation of their chemical constituents. The database consisted of the compound name, molecular formula, accurate molecular mass, chemical structure, MS² mass spectra, and related product ion information. The total ion chromatograms (BPIs) of TSD and the urine and plasma samples after oral administration by UHPLC-Q-Exactive-MS/MS in positive and negative ion modes are presented in Figure 2. It is found that the majority of alkaloids responded well in the positive mode, and the majority of phenolic compounds and saponins responded well in the negative mode. A total of 82 prototype compounds were identified or tentatively characterized, including 41 alkaloids, 35 phenolic compounds, and 6 saponins (shown in Table 2) by comparing the EICs among TSD, drugged, and blank samples and by comparison with reference standards, internal database, and the literature. Figure S3 (Supplementary Materials) displayed MS/MS spectra of major prototype compounds in the urine samples.

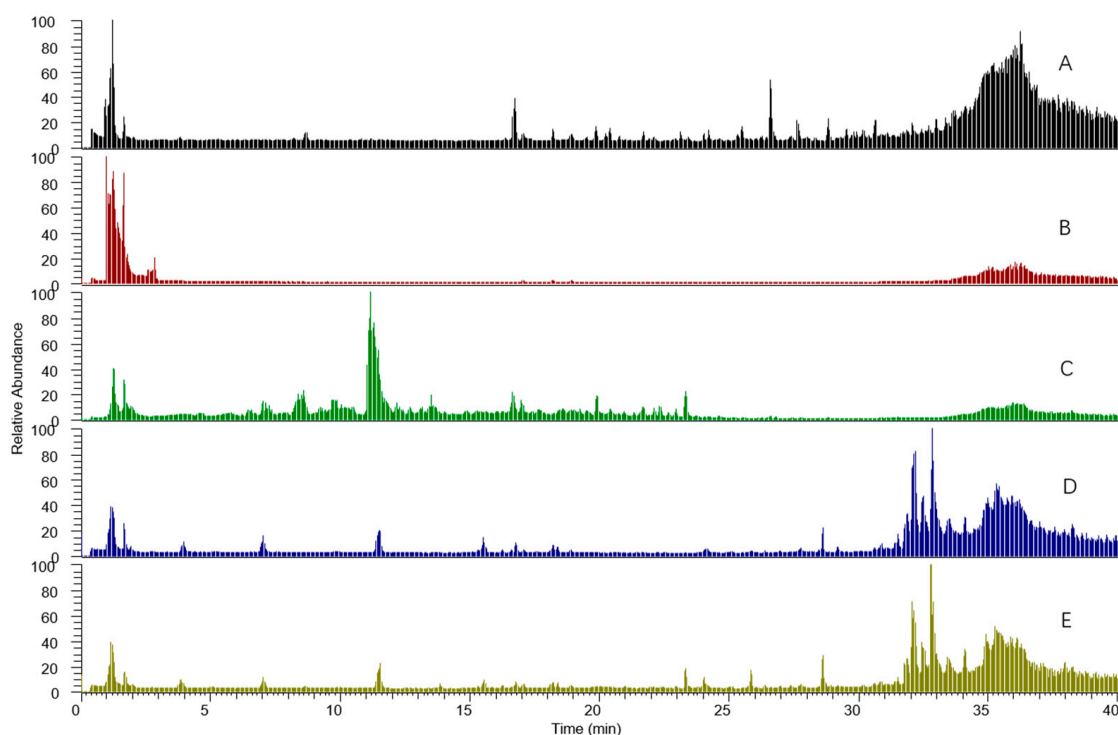


Figure 2. Total ion chromatograms (TIC) of TSD and the urine and plasma samples after oral administration by UHPLC-Q-Exactive-MS/MS ((A): Tongmai Sini decoction; (B): blank urine samples; (C): urine samples; (D): blank plasma samples; (E): plasma samples.).

Table 2. Prototype compounds identified or tentatively characterized in the urine and plasma samples after oral administration of TSD.

ID	[M+H] ⁺ (m/z)	Formula	t _R (min)	Error (ppm)	ms/ms	Identification	ClogP	Area	
								Urine	Plasma
Alkaloids									
1.	394.25839	C ₂₂ H ₃₅ NO ₅	3.51	−1.58	376.2474, 358.2376, 344.2229, 326.2116, 243.2516	Karakolidine		+++	
2.	394.25820	C ₂₂ H ₃₅ NO ₅	4.02	−1.42	376.2476, 358.2367, 340.2268, 328.2260, 307.4473, 218.6333	Chuanfumine		+++	
3.	439.25229 ^{[M-H]⁻}	C ₂₃ H ₃₇ NO ₇	4.25	0.56	392.2438, 344.2226, 295.8235, 193.8604, 146.9375	9-Hydroxysenbusine A		+	
4.	424.26871	C ₂₃ H ₃₇ NO ₆	6.69	−1.55	406.2584, 388.2478, 356.2207, 154.1227	Senbusine A	−2.70	+++	
5.	486.26941	C ₂₄ H ₃₉ NO ₉	7.01	−0.72	454.2438, 436.2322, 404.2069, 378.1887, 372.1793, 319.9836	Mesaconine		++	
6.	424.26871	C ₂₃ H ₃₇ NO ₆	7.74	−1.55	406.2581, 388.2472, 356.2210, 154.1231	Senbusine B	0.16	++	
7.	378.26306	C ₂₂ H ₃₅ NO ₄	8.20	−2.18	360.2524, 342.2431, 328.2268, 242.3140	Karakoline		++	
8.	408.27371	C ₂₃ H ₃₇ NO ₅	8.26	−1.81	390.2631, 372.2533, 358.2367, 340.2271	Isotalatizidine		++	
9.	358.23691	C ₂₂ H ₃₁ NO ₃	9.17	−2.13	340.2265	Songorine		+	
10.	360.25293	C ₂₂ H ₃₃ NO ₃	9.18	−1.09	-	Napelline		++	
11.	330.20569	C ₂₀ H ₂₇ NO ₃	9.70	−2.07	236.8785, 170.7432, 152.4712	Hetisine		++	
12.	470.27435	C ₂₄ H ₃₉ NO ₈	10.51	−1.05	-	Hypaconine		++	
13.	454.27933	C ₂₄ H ₃₉ NO ₇	11.33	−1.26	436.2685, 418.2609, 404.2422, 154.1227	Fuziline		+++	
14.	438.28445	C ₂₄ H ₃₉ NO ₆	11.58	−1.28	420.2736, 402.2617, 388.2472, 356.2214, 278.6899	Neoline		+++	
15.	420.27390	C ₂₄ H ₃₇ NO ₅	12.31	−1.32	402.2632, 384.2512, 370.2359, 342.2414, 324.2322, 251.1396	14-Acetylkarakoline		+	
16.	484.28937	C ₂₅ H ₄₁ NO ₈	12.41	−2.33	-	Deoxyaconine		+	
17.	342.16931	C ₂₀ H ₂₃ NO ₄	12.89	−1.96	297.1120, 282.0887, 237.0910, 219.0804, 191.0860	N-Methyl-laurotetanine		+++	
18.	422.28931	C ₂₄ H ₃₉ NO ₅	13.64	−1.88	390.2629, 372.2517, 358.2379, 340.2238, 98.0970	Talatizamine		++++	++
19.	420.23825	C ₂₃ H ₃₃ NO ₆	15.48	−0.86	402.2268, 370.1989, 293.7002, 154.1224	Giraldine F		++	
20.	452.29996	C ₂₅ H ₄₁ NO ₆	15.54	−1.57	420.2740, 388.2465, 356.2219, 209.1644, 154.1228, 114.0916	Chasmanine		++++	
21.	464.30038	C ₂₆ H ₄₁ NO ₆	16.933	−0.60	432.2740, 414.2626, 400.2474, 372.2535, 265.1608, 235.1487, 154.1225	14-Acetyltalatizamine		++++	++
22.	606.28992	C ₃₁ H ₄₃ NO ₁₁	17.26	−1.60	574.2627, 556.2545, 524.2269, 506.2188, 492.1945, 261.0641, 173.0955, 105.0341	14-Benzoyl-10-OH-mesaconine		++	
23.	544.28955	C ₃₀ H ₄₁ NO ₈	19.47	−0.95	512.2635, 494.2548, 480.2364, 462.2258, 390.2286, 270.0846, 105.0340	Gadenine		+	
24.	590.29490	C ₃₁ H ₄₃ NO ₁₀	19.51	−1.78	558.2616, 540.2575, 419.7593, 307.8019, 246.8854, 105.0339	14-Benzoylmesaconine		++	
25.	540.29486	C ₃₁ H ₄₁ NO ₇	20.01	−1.33	504.2730, 462.2614, 382.2463, 340.2256, 322.2149, 304.2042	Aconicarchamine B		+	
26.	604.31060	C ₃₂ H ₄₅ NO ₁₀	20.53	−1.68	572.2811, 554.2750, 522.2495, 490.2176, 340.3151, 105.0341	14-Benzoylaconine		++	
27.	574.30010	C ₃₁ H ₄₃ NO ₉	21.20	−1.65	542.2744, 510.2461, 304.5384, 198.1281, 105.0339	14-Benzoylhypaconine		+++	
28.	618.29210 ^{[M-H]⁻}	C ₃₂ H ₄₅ NO ₁₁	21.21	0.31	384.9167, 351.8983, 270.7405, 190.9267	14-Benzoyl-10-OH-aconine		++	
29.	648.30023	C ₃₃ H ₄₅ NO ₁₂	21.93	−1.98	588.2775, 556.2513, 455.3509, 370.1645, 105.0340	10-OH-mesaconitine		++	

Table 2. Cont.

ID	[M+H] ⁺ (m/z)	Formula	t _r (min)	Error (ppm)	ms/ms	Identification	ClogP	Area	
								Urine Plasma	
30.	558.30530	C ₃₁ H ₄₃ NO ₈	22.07	−1.52	526.2800, 508.2674, 232.0710182.0626, 105.0341	14-Benzoyl-doxyhyapaconine		++	
31.	588.31561	C ₃₂ H ₄₅ NO ₉	22.32	−1.24	556.2905, 524.2639, 506.2443, 346.4250, 253.7027, 154.1226, 105.0341	14-Benzoyldeoxyaconine		+	
32.	542.31061	C ₃₁ H ₄₃ NO ₇	23.18	−1.15	510.2846, 492.2735, 482.2483, 460.2504, 154.1231	14-Benzoylneoline		+	
33.	632.30591	C ₃₃ H ₄₅ NO ₁₁	23.18	−0.63	572.2844, 540.2551, 522.2487, 508.2299, 354.1694, 105.0341	Mesaconitine *		+++	
34.	662.31683	C ₃₄ H ₄₇ NO ₁₂	23.39	−0.27	-	Aconifine		++	
35.	614.29553	C ₃₃ H ₄₃ NO ₁₀	24.17	−0.72	554.2743, 494.2534, 372.2162, 344.21622, 203.5583, 105.0341	2,3-didehydrohyapaconitine		+	
36.	646.32135	C ₃₄ H ₄₇ NO ₁₁	24.58	−0.84	586.3002, 554.2727, 526.2797, 494.2520, 368.1843, 105.0340	Aconitine *		++	
37.	616.31079	C ₃₃ H ₄₅ NO ₁₀	24.61	−0.83	556.2903, 524.2634, 496.2750, 464.2434, 338.1741, 310.1812, 105.0341	Hypaconitine *		++++	
38.	600.31592	C ₃₃ H ₄₅ NO ₉	24.96	−1.32	540.2948, 508.2683, 480.2747, 476.2424, 448.2475, 354.2031, 254.4337, 105.0339	Secoyunaconitine		+	
39.	572.32117	C ₃₂ H ₄₅ NO ₈	24.95	−1.10	484.2688, 456.2745, 382.2002, 322.1798, 294.1857, 158.0964	14-O-Anisoyleoline		+	
40.	630.32635	C ₃₄ H ₄₇ NO ₁₀	26.07	−1.36	570.3046, 538.2788, 510.2882, 506.2528, 478.2571, 352.1898, 314.5361, 105.0341	3-Deoxyaconitine		+++	
41.	614.33173	C ₃₄ H ₄₇ NO ₉	27.60	−0.53	-	Chasmaconitine		++	
Phenolic compounds									
42.	209.04474 ^{[M-H][−]}	C ₁₀ H ₁₀ O ₅	8.56	−3.85	165.0545, 121.0281, 103.9187, 87.9238, 59.0123	Hydroxyferulic acid		+++	++
43.	433.13394 ^{[M-H][−]}	C ₁₈ H ₂₄ O ₁₂	9.88	0.08	161.0442, 125.0230, 99.0436	Asperulosidic acid		++	
44.	433.11407 ^{[M-H][−]}	C ₂₁ H ₂₂ O ₁₀	13.87	−0.19	271.0615, 151.0024	5-Hydroxyliquiritin		++	
45.	593.15137 ^{[M-H][−]}	C ₂₇ H ₃₀ O ₁₅	15.51	0.29	473.1098, 383.9785, 353.0774	Vitexin II		+++	
46.	563.14055 ^{[M-H][−]}	C ₂₆ H ₂₈ O ₁₄	15.83	−0.51	473.1089, 443.0985, 383.0769, 253.0502, 146.9367	Vitexin I		+	
47.	417.11890 ^{[M-H][−]}	C ₂₁ H ₂₂ O ₉	16.74	−0.32	255.0662, 153.0182, 135.0074, 119.0488	Liquiritin *		++++	
48.	505.13339	C ₂₄ H ₂₄ O ₁₂	18.72	−0.89	257.0809, 137.0234	Malonyl liquiritin		+	
49.	505.13358	C ₂₄ H ₂₄ O ₁₂	18.99	−0.07	257.0810, 137.0234	Malonyl liquiritin		+	
50.	431.13280	C ₂₂ H ₂₂ O ₉	20.26	−1.97	269.0809	Ononin		++++	
51.	417.11908 ^{[M-H][−]}	C ₂₁ H ₂₂ O ₉	20.39	−1.01	255.0662, 153.0180, 135.0072, 119.0481	Neoliquiritin	0.75	+++	
52.	417.11900 ^{[M-H][−]}	C ₂₁ H ₂₂ O ₉	20.74	−2.47	255.0662, 153.01816, 135.0074, 119.0488	Isoliquiritin	1.28	++	
53.	285.07670 ^{[M-H][−]}	C ₁₆ H ₁₄ O ₅	21.23	−0.31	270.0536, 253.0505, 177.0182, 150.0310, 108.0203	Licochalcone B		++	
54.	255.06560	C ₁₅ H ₁₀ O ₄	21.30	0.10	227.0704, 199.0754, 145.0286, 137.0234	Dihydroxyflavone		++++	
55.	255.06580 ^{[M-H][−]}	C ₁₅ H ₁₂ O ₄	21.70	−0.36	153.0180, 135.0073, 119.0487, 91.0173	Liquiritigenin *		++++	+++
56.	295.19040	C ₁₇ H ₂₆ O ₄	23.34	−0.22	177.0914, 163.0755, 137.0598, 131.0493, 99.0809	6-Gingerol		++++	++
57.	269.04530 ^{[M-H][−]}	C ₁₅ H ₁₀ O ₅	24.34	0.38	233.1537, 181.0644	Genistein		+++	
58.	255.06586 ^{[M-H][−]}	C ₁₅ H ₁₂ O ₄	26.29	−0.49	153.0179, 135.0073, 119.0487, 91.0174	Isoliquiritigenin *		++++	+++

Table 2. Cont.

ID	[M+H] ⁺ (m/z)	Formula	t _R (min)	Error (ppm)	ms/ms	Identification	ClogP	Area	
								Urine Plasma	
59.	269.08170	C ₁₆ H ₁₂ O ₄	26.58	1.04	253.0497, 237.0554, 213.0911, 118.0418, 107.0497	Formononetin *		++++	+++
60.	367.11790 ^{[M-H]⁻}	C ₂₁ H ₂₀ O ₆	27.75	-1.99	352.0944, 309.0400, 298.0476, 283.0247	Glycycoumarin/Licocoumarione		+++	
61.	271.09565	C ₁₆ H ₁₄ O ₄	28.56	1.19	254.2579, 161.0599, 137.0598, 123.04440, 100.0763	Echinatin		++	
62.	355.11835 ^{[M-H]⁻}	C ₂₀ H ₂₀ O ₆	28.60	-1.07	328.1265, 269.11820, 269.11820, 178.9975, 125.0230	8-Dimethylallyleriodictyol/6-Dimethylallyleriodictyol		++	
63.	277.18008	C ₁₇ H ₂₄ O ₃	28.84	2.28	177.0912, 145.0649, 137.0598	6-Shogaol		+++	++
64.	355.15480 ^{[M-H]⁻}	C ₂₁ H ₂₄ O ₅	29.81	-1.06	323.1284, 233.1176, 207.1017, 135.0438, 125.0230, 109.0280	Isopentadienyl glycyrrhizoflavone		++	
65.	367.11790 ^{[M-H]⁻}	C ₂₁ H ₂₀ O ₆	29.53	-2.00	309.0400, 297.0400, 284.0325, 203.0702	Glycycoumarin/Licocoumarione		+++	
66.	321.11262 ^{[M-H]⁻}	C ₂₀ H ₁₈ O ₄	30.07	-1.93	306.0892, 174.9549	Licoflavone A		+	
67.	353.10290 ^{[M-H]⁻}	C ₂₀ H ₁₈ O ₆	30.17	-1.33	339.1187, 321.1126, 295.0613, 283.0614, 270.0535	Isolicoflanonol		+++	++
68.	353.13782	C ₂₁ H ₂₀ O ₅	30.22	-1.59	299.0906, 297.0857, 267.0653, 199.0758, 147.0441, 135.0441	Gancaonin M		++	
69.	383.11273 ^{[M-H]⁻}	C ₂₁ H ₂₀ O ₇	30.39	-2.33	338.2439, 247.1310, 227.0704, 207.1015, 155.0337, 140.0101	Licopyranocoumarin		+	
70.	383.14828	C ₂₂ H ₂₂ O ₆	30.66	-1.50	327.0859, 299.0913, 191.0704	Glycyrin		++	++
71.	355.15320	C ₂₁ H ₂₂ O ₅	30.94	-2.01	289.0549, 287.0553, 191.1067, 153.0548, 69.0708	Licobenzofuran/liconeolignan		+++	
72.	337.10780 ^{[M-H]⁻}	C ₂₀ H ₁₈ O ₅	31.02	-1.07	314.0428, 282.0531	Licoflavone C		++	
73.	365.10239 ^{[M-H]⁻}	C ₂₁ H ₁₈ O ₆	30.17	-1.63	307.0244, 295.0245, 282.0169	Isoglycyrol	4.84	++	
74.	365.10236 ^{[M-H]⁻}	C ₂₁ H ₁₈ O ₆	31.12	-1.99	307.0242, 295.0243, 282.0167	Glycyrol	5.04	+++	
75.	333.24170	C ₂₁ H ₃₂ O ₃	34.17	-1.99	177.0911, 145.0649, 137.0598	10-Shogaol		++	
76.	279.23264 ^{[M-H]⁻}	C ₁₈ H ₃₂ O ₂	38.27	1.13	261.2219, 199.8500	Linoleic acid		++	
Saponins									
77.	879.40173 ^{[M-H]⁻} 881.41516 705.38361 ^{[M+H-glcA]⁺} 511.34122 ^{[ag⁺+H-H₂O]⁺}	C ₄₄ H ₆₄ O ₁₈	24.011	-0.67 -1.38	(-) 351.0557, 193.0342, 113.0229 (+) 511.3408, 493.3279, 451.3188, 141.0183	Uralsaponin M		++	
78.	837.39105 ^{[M-H]⁻} 839.40466 469.33072 ^{[gal+H-H₂O]⁺} 837.39178 ^{[M-H]⁻}	C ₄₂ H ₆₂ O ₁₇	25.49	-0.79 -1.32	(-) 351.05603, 289.05652, 193.03430, 175.02340, 113.02294 (+) 469.3304, 487.3415, 451.3209, 141.0184	Yunganoside K2		++	
79.	839.40491 469.33084 ^{[ag⁺+H-H₂O]⁺}	C ₄₂ H ₆₂ O ₁₇	26.07	-0.84 -1.07	(-) 351.05557, 289.05621, 193.03413, 175.02360, 113.02285 (+) 469.3304, 487.3413, 451.3198, 141.0183	Licoricesaponin G2		+	

Table 2. Cont.

ID	[M+H] ⁺ (m/z)	Formula	t _R (min)	Error (ppm)	ms/ms	Identification	ClogP	Area Urine Plasma
80.	471.34613	C ₃₀ H ₄₆ O ₄	26.62	−1.41	453.33508, 425.34262, 317.21100, 235.16887, 189.16374	Glycyrrhetic acid (enoxolone) *		+
81.	821.39630 ^{[M-H]⁻} 823.40936 647.37744 ^{[M+H-glcA]⁺} 453.33554 ^{[agl+H-H2O]⁺}	C ₄₂ H ₆₂ O ₁₆	26.64	1.08 −1.70	(−) 351.05573, 193.03406, 175.02338, 113.02288 (+) 453.3354, 471.3451, 435.3259	Glycyrrhizic acid *		++++
82.	821.39612 ^{[M-H]⁻} 823.40936 647.37787 ^{[M+H-glcA]⁺} 453.33585 ^{[agl+H-H2O]⁺}	C ₄₂ H ₆₂ O ₁₆	27.65	0.86 −0.47	(−) 351.05640, 193.03404, 175.02319, 113.02289 (+) 453.3354, 435.3257	Uralsaponin B or Licoricesaponine K2/H2		++

Note: * Compounds identified by comparing with reference standards; glcA: β-D-glucuronopyronosyl; agl: aglycone; +, response area below 10⁶; ++, response area between 10⁶ and 10⁷; +++, response area between 10⁷ and 10⁸; +++++, response area above 10⁸.

3.2.1. Identification of Alkaloid Components

Metabolites for alkaloids obtained in this study could be classified into three subtypes, namely, diester-diterpenoid alkaloids (DDAs), monoester-diterpenoid alkaloids (MDAs), and amine-diterpenoid alkaloids (ADAs) [30]. We conducted an in-depth study of the chemical constituents of alkaloids of *Aconitum carmichaeli* in previous research [24,29], in which we carried out detailed mass fragmentation analysis of DDAs, MDAs, and ADAs, and a total of 42 DDAs and 120 diterpenoid alkaloids were identified, respectively.

In the MS² spectra of DDAs, the most abundant ion yielded from the loss of a molecule of AcOH at the C₈ site, which could be a diagnostic neutral loss for the differentiation of DDAs from MDAs and ADAs [29]. Thus, Compounds 29, 33, 35–38, and 40–41 were extracted by NLF for 60 Da in MS spectra for the urine sample, showing their molecular weight between 600 and 650 Da. Among them, Compounds 33, 36, and 37 were unambiguously identified as mesaconitine (MA), aconitine (AC), and hypaconitine (HA), respectively, by comparing their t_R values and mass spectra data with those of reference compounds. Apart from the ion of [M+H-60(AcOH)]⁺ (*m/z* 572.2844, 586.3002, 556.2903), the ions of [M+H-60-32(MeOH)]⁺ (*m/z* 554.2727, 524.2634, 540.2551) and [M+H-60-32(MeOH)-28(carbonyl group)]⁺ (*m/z* 526.2797, 496.2750, 522.2487) of the three compounds, respectively, suggested the active elimination of MeOH occurred at C16 site and a neutral molecule of CO, which could also be regarded as characteristic fragments for identification of the DDAs. Compounds 29, 35, 38, and 40–41 were tentatively identified as 10-OH-mesaconitine, dehydrohypaconitine, secoyunaconitine, 3-deoxyaconitine, and chasmaconitine by comparing their acquired accurate mass data, characteristic fragment ions with those of compounds in our previous research [29].

In the MS spectra for the urine sample, by extraction of NLF for both 32 Da and 18 Da with limitation of molecular weight ranging from 500 to 620 Da, ten peaks were found. Neutral losses of 32, 18, and 122 Da, corresponding to the elimination of acetic acid, methanol, and benzoic acid, or combinations of these, could be considered diagnostic fragment ions for MDAs [31]. However, fragment peaks formed by the loss of the typical substituent group as BzOH (122 Da) were hardly detected for MDAs in this study. Thus, Compounds 22–28 and 30–32 were identified as MDAs accordingly by comparing the accurate mass data and diagnostic fragment ions with those of the compounds in our previous research [24].

A total of 21 prototype compounds were identified as ADAs, most of which possessed molecular weight between 390 and 500 Da and were eluted within the initial 16 min. The substitutions of C₁ and C₃ sites of ADAs were relatively active sites and could be easily cleaved, yielding major peaks [M+H-H₂O]⁺ or [M+H-CH₃OH]⁺ in MS² spectra as the diagnostic ion accordingly. Fragmentation pathways of differently substituted ADAs included different diagnostic ions. Compounds 1, 4, 6, 7, 8, 13, 14, as ADAs with C₁-OH substitution, firstly fragmented into [M+H-H₂O]⁺ as diagnostic fragment ions and followed by losses of typical substituent groups (CH₃OH and H₂O) in their MS² spectra. By comparing their accurate mass data with our chemical database and the literature [24,32], they were identified as karakolidine, senbusine A, senbusine B, karakoline, isotalatizidine, fuziline, and neoline, respectively. For Compounds 18 (talatizamine), the most prominent fragmentation ions were designated as 390.2696 ([M+H-CH₃OH]⁺), suggesting its C₁ site with -OCH₃ substitutions. It also yielded 372.2517 ([M+H-CH₃OH-H₂O]⁺), 358.2379 ([M+H-CH₃OH-CH₃OH]⁺), and 340.2238 ([M+H-CH₃OH-CH₃OH-H₂O]⁺), and its characteristic fragmentation patterns are shown in Figure 3.

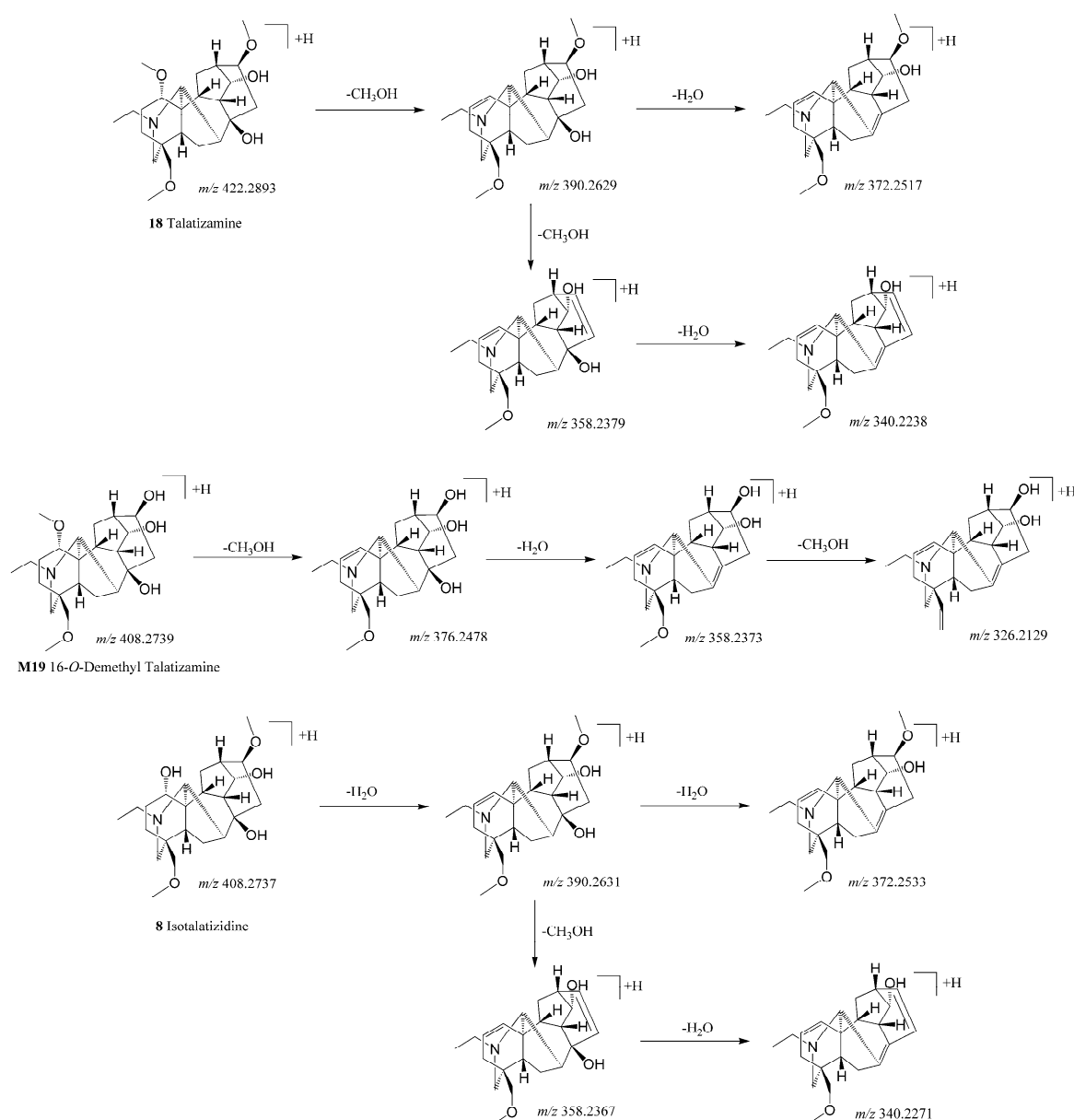


Figure 3. Probable fragmentation pathways of talatizamine, isotalatizidine, and 16-O-demethyl talatizamine.

3.2.2. Identification of Phenolic Compounds

In addition to alkaloids from RALP, the main prototype compounds identified *in vivo* included flavonoids, isoflavonoids, coumarins, and saponins from RGP, and volatile oils from RZ, as shown in Table 2. The MS data of these compounds were compared with those of reference standards, internal databases, and the literature, while isomers could be initially identified by comparing their ClogP.

Flavonoids are important active components of RGP, among which four components, namely liquiritigenin, isoliquiritigenin, iquiritin, and isoliquiritin, have the highest content and are regarded as the indicator components of RGP, which were identified by comparing mass data with those of the reference standards. Compound 47, as reference compound liquiritin, formed the $[M-H]^-$ -based peak at m/z 417.11890 ($C_{21}H_{21}O_9^-$), for which furtherly formed fragmentation ion m/z 255.0662 $[M-H-glu]^-$ of the aglycone element in the MS/MS spectrum, accompanied by three characteristic fragments at m/z 135.0074

($C_7H_3O_3^-$), 119.0488 ($C_8H_7O^-$), and 91.0173 ($C_6H_3O^-$), which can be used for the identification of the same type of licorice flavonoids.

Compound **50** formed the $[M+H]^+$ molecular ion peak at m/z 431.13280 and further removed one molecule of glucose residues to form the aglycone at m/z 269.08121, which was identified as ononin, the main isoflavone of RGP. Its aglycone formed the same ion at m/z 269.08170 at the retention time of 26.58 min and was fragmented into the fragments of m/z 253.0497, 237.0554, and 213.0911, which is identified as formononetin, and the two prototypes are the most important isoflavonoid components in RGP.

The elemental compositions of other types of licorice flavonoid constituents determined by LC-MS were compared with the data of existing database compounds. Compounds **44**, **53**, **54**, **67**, and **68** were preliminarily identified as 5-hydroxyliquiritin, licochalcone B, dihydroxyflavone, licoflavone A, and isolicoflanonol. Similarly, other types of phenolic compounds, such as coumarins, were identified or preliminarily identified, including Compounds **60**, **66**, **64**, **70**, **73**, and **74**, which were identified as glycycomarim, licocoumarone, licopyranocoumarin, glycyrin isoglycyrol, and glycyrol, correspondingly. A few other phenolic components observed in vivo of TSD were derived from RZ, while compounds **56**, **63**, and **75** were tentatively identified as 6-gingerol, 6-shogaol, and 10-shogaol, respectively, with fragment ions m/z 177.09 and 137.06 as their characteristic fragment ions in PI mode, which is consistent with the literature [33].

3.2.3. Identification of Saponins

From the LC-MS/MS profiles, six saponin components were found as absorbed prototype components, all of which were derived from RGP. The saponins (Compounds **77**, **78**, **79**, **81**, and **82**) were within the retention time of 14–21 min and had both mass spectral response in NI and in PI mode.

As a general rule for triterpenoid saponins in MS/MS spectra, the fragmentation reactions undergone by activated saponin ions almost occur within the glycan part of the saponin ions, and the sugar chains can be eliminated successively from end to inner and finally to obtain an aglycone ion [34]. Through glycosidic cleavages or cross-ring cleavages, the parent ion obtained a series of ions retaining the charge at the reducing terminus were termed Y and Z (glycosidic cleavages) and X (cross-ring cleavages), whereas those ions retaining the charge at the non-reducing terminus are termed B, C (glycoside cleavages), and A (cross-ring cleavages) [35].

The MS cleavage pathways of saponins from RGP, however, were incompletely abided by this rule. Take glycyrrhizic acid as an example; in MS spectra of PI mode, the ions of $[M-H]^-$ were obtained, accompanied by the fragment ions of m/z 647.37744 $[M+H-\beta-D\text{-glucuronopyronosyl (glcA)}]^+$ and m/z 453.33554 $[\text{aglycottonne (agl)}+H-H_2O]^+$, which were similarly for the other detected saponins and has not been reported up to present. More interestingly, in the MS/MS spectra of the detected saponins, the ions of $[\text{agl}+H-H_2O]^+$ rather than $[\text{agl}+H]^+$ were observed as the base peaks, namely, m/z 453.34 ($C_{30}H_{45}O_3^+$), 469.33 ($C_{30}H_{45}O_4^+$), and 511.34 ($C_{30}H_{45}O_4^+$), corresponding to the aglycone of enoxolone, hydroxyenoxolone, and acetoxenoxolone, respectively.

The produced ions obtained in NI mode were quite different from those in PI mode. The fragment ions of glycosidic cleavages or cross-ring cleavages, as well as the aglycone, were hardly detected in NI mode. The ions of m/z 351.05 ($C_{12}H_{15}O_{12}^-$), 193.03 ($C_6H_9O_7^-$), 175.02 ($C_6H_7O_6^-$), and 113.02 ($C_5H_5O_3^-$) were observed, corresponding to the successive loss of two glucuronopyranosyls. Thus, the identification information for aglycone s and sugar chains of licorice saponins can be obtained from PI and NI ion modes, respectively.

3.3. Identification of Metabolites

Prototypes and metabolites exist simultaneously in plasma and urine samples. Thirty-two major prototypes, including 11 alkaloids from RALP, as well as 21 phenolic and saponin compounds from RGP and RZ, were selected as MDF templates for metabolite screening. The 32 compounds contained a wide range of chemical structure types with relatively

high content in TDS. A total of 40 alkaloids and 25 phenolic compounds were identified or tentatively characterized by comparing the mass data with those of prototype compounds and metabolic pathways reported by the literature [36–40].

After prototypes are absorbed into the body, some of them are excreted as prototypes, and some of them can be converted into other metabolites. DDAs were ester hydrolyzed to MDAs in rats; for example, MA, HA, and AC could be ester hydrolyzed to 14-Benzoylmesaconine (BM), 14-Benzoylhypaconine (BH), and 14-Benzoylaconitine (BA) during the process of metabolism in rat, while BM, BH, and BA themselves could be metabolized to mesaconine, hypaconine, and aconine [36]. Therefore, certain prototypes are themselves metabolites and metabolized from other prototypes in rats.

3.3.1. Identification of Alkaloid Metabolites

For diterpenoid alkaloids, most metabolites from hydroxylation, deoxygenation, demethylation, deethylation, dehydrogenation, ester hydrolysis, and demethylation with deoxygenation have been found in vivo. Metabolites of alkaloids were identified or tentatively identified based on their metabolic pathways, as reported in the literature [37].

The metabolites for major alkaloids were found in the urine and plasma samples, as displayed in Table 3. Most metabolites observed were mainly metabolized from karakolidine, songorine, karakoline, talatizamine, hypaconitine, mesaconitine, neoline, and fuziline. These results manifested that alkaloids mainly underwent oxidation, dehydrogenation, demethylation, N-deethylation, hydrolysis, demethylation with deoxygenation, and dehydrogenation with demethylation, etc.

After oral administration of TSD, eight related metabolites of talatizamine (**18**) were identified in urine samples. Metabolite **M18** and **M19** showed $[M+H]^+$ ion at m/z 408.27386 and 408.27393 (giving formula $C_{23}H_{37}NO_5$), 14 Da (CH_2) less than the parent compound. In the MS^2 spectra, characteristic ions at m/z 376.25 ($[M+H-CH_3OH]^+$), 358.24 ($[M+H-CH_3OH-H_2O]^+$), and 326.21 ($[M+H-CH_3OH-H_2O-CH_3OH]^+$), suggesting its C_1 site with $-OCH_3$ substitutions. Those characteristic ions were different from the characteristic ions of the prototype component, isotalatizidine (Compound **8**), although they shared the same elemental composition ($C_{23}H_{37}NO_5$). Isotalatizidine, with $-OH$ substitutions at the C_1 site, first yielded 390.2631 ($[M+H-H_2O]^+$) by loss of H_2O at the C_1 site. The fragmentation pathways of demethyl talatizamine and isotalatizidine can be compared in Figure 3. The methyl group of the C_{16} site or C_{18} site could easily be metabolized instead of that of the C_1 site for **M18** and **M19**. The Clog p values of 18-*O*-demethyl talatizamine and 16-*O*-demethyl talatizamine were -0.78 and -0.74 , calculated by ChemDraw 14.0. Hence, **M18** and **M19** were tentatively determined as 18-*O*-demethyl talatizamine and 16-*O*-demethyl talatizamine.

M4 was confirmed as hydroxylated talatizamine for the $[M+H]^+$ ion at m/z 438.28433 (formula $C_{24}H_{39}NO_6$), 16 Da (O) more than talatizamine, and the fragment ions at m/z 406.2588, 388.2476, 374.230 and 356.2226 were all 16 Da less than those of talatizamine. Therefore, **M4** was deduced as 10-Hydroxy Talatizamine, as for the C_{10} site in diterpenoid alkaloids prone to be hydroxylated by the literature [38].

Apart from these three metabolites, other metabolites (**M13**, **M26**, **M36**, **M39**, and **M40**) of talatizamine were produced through the reaction of dehydrogenation, demethylation, N-deethylation, and deoxygenation. The proposed metabolic pathways of talatizamine are shown in Figure 4. The other metabolites of alkaloids were deduced accordingly by their acquired accurate mass data, retention time, and characteristic fragment ions, as well as the Clog p values, and biotransformation pathways information and composition change calculated by ChemDraw 14.0 and Compound Discoverer 3.2.

Table 3. Metabolites of major alkaloids found in the urine and plasma samples.

ID	[M+H] ⁺ (m/z)	Formula	t _R (min)	Error (ppm)	ms/ms	Composition Change	Identification	ClogP	Area	
									Urine	Plasma
M1.	410.25302	C ₂₂ H ₃₅ NO ₆	3.72	−1.69	392.2425, 374.2317, 360.2165, 342.2054	+O	Hydroxy karakolidine		++	
M2.	374.23212	C ₂₂ H ₃₁ NO ₄	7.55	−1.25	356.2212, 338.2106, 198.1122	+O	Hydroxy songorine		++	
M3.	394.25812	C ₂₂ H ₃₅ NO ₅	7.76	−1.85	376.2476, 358.2362, 98.0971, 58.0611	+O	Hydroxy karakoline		++	
M4.	438.28433	C ₂₄ H ₃₉ NO ₆	10.76	0.67	406.2588, 388.2476, 374.230, 356.2226	+O	10-Hydroxy talatizamine		++	
M5.	632.30560	C ₃₃ H ₄₅ NO ₁₁	22.61	−1.50	572.2853, 540.2590, 512.2641, 508.2310, 480.2390, 358.2004, 354.1703, 105.0341	+O	Hydroxy hypaconitine		++	
M6.	392.24268	C ₂₂ H ₃₃ NO ₅	8.28	−1.21	374.2315, 344.2221, 312.1962, 114.0916	-H2	Dehydrogenated karakolidine		+++	
M7.	392.24249	C ₂₂ H ₃₃ NO ₅	8.95	−2.15	374.2325, 344.2240	-H2	Dehydrogenated karakolidine		+++	
M8.	452.26361	C ₂₄ H ₃₇ NO ₇	9.85	−1.48	434.2529, 416.2419, 204.2270, 384.2155	-H2	Dehydrogenated fuziline		+++	
M9.	376.24780	C ₂₂ H ₃₃ NO ₄	10.38	−1.82	358.2373, 98.0969	-H2	Dehydrogenated karakoline		++	
M10.	376.24756	C ₂₂ H ₃₃ NO ₄	10.96	−1.15	358.2375, 234.0137, 98.0970	-H2	Dehydrogenated karakoline		+++	
M11.	436.26895	C ₂₄ H ₃₇ NO ₆	10.24	−0.95	418.2581, 400.2475, 386.2315, 358.2355, 340.2265	-H2	Dehydrogenated neoline		+++	+
M12.	436.26907	C ₂₄ H ₃₇ NO ₆	10.64	−0.67	418.2585, 400.2473, 386.2303, 358.2383	-H2	Dehydrogenated neoline		+++	
M13.	420.27393	C ₂₄ H ₃₇ NO ₅	13.60	−1.33	388.2477, 370.2375, 98.0972	-H2	14-Dehydrogenated talatizamine		+++	
M14.	364.24744	C ₂₁ H ₃₃ NO ₄	7.39	−2.20	346.2374, 328.2268	-CH2	Demethyl karakoline		+++	+
M15.	364.24740	C ₂₁ H ₃₃ NO ₄	7.86	−2.20	346.2370, 328.2266	-CH2	Demethyl karakoline		++++	+
M16.	424.26892	C ₂₃ H ₃₇ NO ₆	10.68	−1.05	406.2583, 374.2327, 356.2211, 342.2069, 154.1226	-CH2	Demethyl neoline		+++	+
M17.	424.26890	C ₂₃ H ₃₇ NO ₆	11.08	−0.98	406.2581, 374.2317, 356.2222, 342.2076, 154.1228	-CH2	Demethyl neoline		++++	
M18.	408.27386	C ₂₃ H ₃₇ NO ₅	9.87	−1.44	376.2475, 358.2365, 326.2136	-CH2	18- <i>o</i> -Demethyl talatizamine	−0.78	++++	++
M19.	408.27393	C ₂₃ H ₃₇ NO ₅	11.17	−1.29	376.2478, 358.2373, 326.2129	-CH2	16- <i>o</i> -Demethyl talatizamine	−0.73	++++	++
M20.	602.29486	C ₃₂ H ₄₃ NO ₁₀	21.31	−1.70	542.2742, 510.2477, 482.2540, 478.2212, 324.1592, 105.0339	-CH2	Demethyl hypaconitine		++++	+
M21.	618.28992	C ₃₂ H ₄₃ NO ₁₁	22.17	−1.22	558.2684, 526.2423, 508.2394, 354.1695, 105.0341	-CH2	Demethyl mesaconitine		++	
M22.	330.20581	C ₂₀ H ₂₇ NO ₃	8.19	−1.70	312.1954	-C2H4	Deethyl songorine		+++	
M23.	350.23181	C ₂₀ H ₃₁ NO ₄	9.05	−2.21	332.2215, 314.2106, 300.1958, 234.9901, 158.9743	-C2H4	Deethyl karakoline		+++	
M24.	410.25314	C ₂₂ H ₃₅ NO ₆	10.97	−1.40	392.2423, 378.2271, 360.2163, 328.1906	-C2H4	Deethyl neoline		++	
M25.	408.27374	C ₂₃ H ₃₇ NO ₅	8.96	−1.74	390.2631, 372.2537, 358.2369	-CH2O	Demethyl-deoxy neoline		++++	++
M26.	392.27896	C ₂₃ H ₃₇ NO ₄	13.38	−1.46	360.2527, 342.2436, 328.2265	-CH2O	16-O-Demethyl-14-deoxy Talatizamine		+++	
M27.	602.29529	C ₃₂ H ₄₃ NO ₁₀	23.87	−1.20	542.2773, 510.2486, 478.2222, 324.1592, 105.0341	-CH2O	Demethyl-deoxy mesaconitine		+++	
M28.	360.25272	C ₂₂ H ₃₃ NO ₃	9.38	−1.68	342.2422, 324.2325, 121.0651	-H2O	Dehydrated karakoline		+++	+
M29.	360.25250	C ₂₂ H ₃₃ NO ₃	9.92	−2.11	342.2422, 324.2307	-H2O	Dehydrated karakoline		++++	+

Table 3. Cont.

ID	[M+H] ⁺ (m/z)	Formula	t _R (min)	Error (ppm)	ms/ms	Composition Change	Identification	ClogP	Area	
									Urine	Plasma
M30.	614.2517	C ₃₃ H ₄₃ NO ₁₀	24.17	−1.57	544.2743, 522.2518, 494.2534, 372.2162, 344.2215	-H ₂ O	Dehydrated mesaconitine		++	
M31.	380.24277	C ₂₂ H ₃₃ NO ₅	8.81	−1.01	362.2316, 344.2046, 330.2065	-CH ₂ +O	Demethyl-hydroxy karakoline		++	
M32.	438.24811	C ₂₃ H ₃₅ NO ₇	12.09	−1.06	420.2374, 402.2265, 392.2440, 374.2317	-CH ₂ -H ₂	Dehydrogenated-demethyl fuziline		++	+
M33.	438.24890	C ₂₃ H ₃₅ NO ₇	12.21	0.49	420.2367, 402.2283, 392.2442, 374.2323	-CH ₂ -H ₂	Dehydrogenated-demethyl fuziline		++	+
M34.	362.23172	C ₂₁ H ₃₁ NO ₄	8.15	−0.45	344.2223, 185.0710	-CH ₂ -H ₂	Dehydrogenated-demethyl karakoline		+++	
M35.	422.25327	C ₂₃ H ₃₅ NO ₆	10.99	−1.07	390.2268, 406.2597, 390.2268, 374.2324	-CH ₂ -H ₂	Dehydrogenated-demethyl neoline		+++	+
M36.	406.25839	C ₂₃ H ₃₅ NO ₅	10.70	−1.01	388.2477, 370.2368, 328.2266	-CH ₂ -H ₂	14-Dehydrogenated-16-O-demethyl talatizamine		+++	
M37.	346.20090	C ₂₀ H ₂₇ NO ₄	7.79	−1.12	328.1904, 296.1645, 268.1701, 251.1437	-C ₂ H ₄ +O	N-Deethyl-hydroxy songorine		++	+
M38.	346.20071	C ₂₀ H ₂₇ NO ₄	8.49	−1.65	328.1903, 296.1650, 268.1699, 251.1429	-C ₂ H ₄ +O	N-Deethyl-hydroxy songorine		+++	
M39.	378.26337	C ₂₂ H ₃₅ NO ₄	10.98	−1.43	346.2371, 328.2279	-C ₂ H ₄ -O	N-Deethyl-14-deoxy talatizamine	0.88	+++	+
M40.	378.26334	C ₂₂ H ₃₅ NO ₄	11.23	−1.45	346.2371, 328.2267	-C ₂ H ₄ -O	N-Deethyl-8-deoxy talatizamine	1.15	+++	

Note: +, response area below 10⁶; ++, response area between 10⁶ and 10⁷; +++, response area between 10⁷ and 10⁸; +++++, response area above 10⁸.

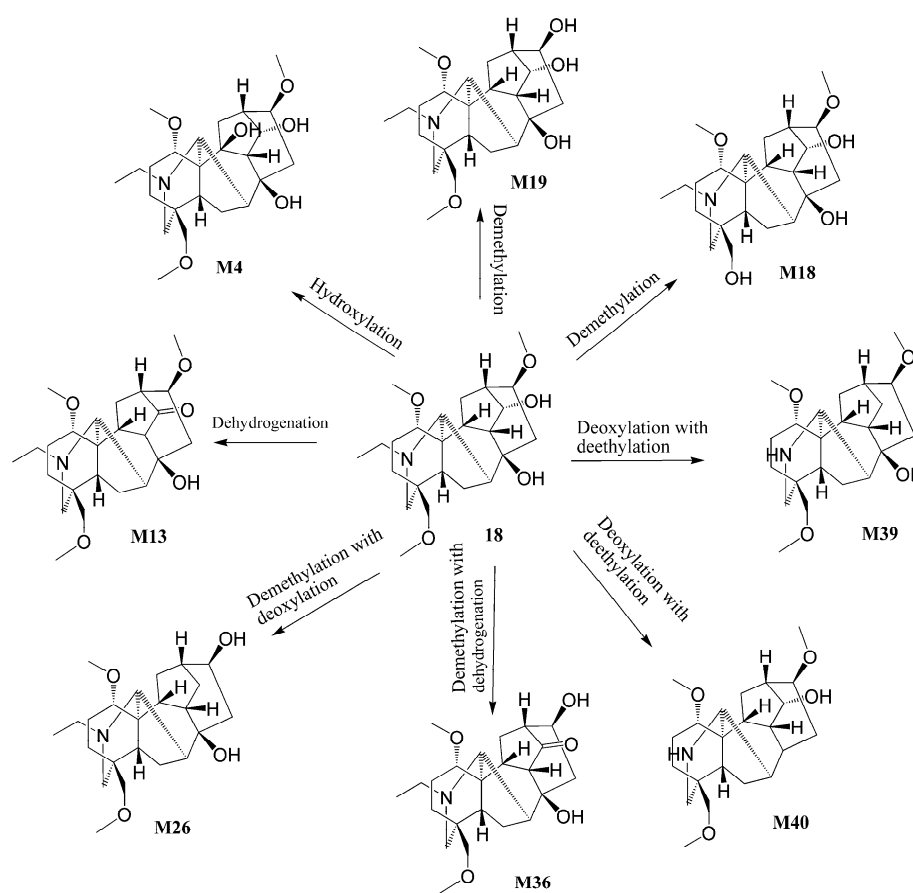


Figure 4. Proposed metabolic pathways of talatizamine in vivo.

3.3.2. Identification of Phenolic Compound Metabolites

Metabolites of phenolic compounds, mainly from hydroxylation, oxylation, methylation, dehydrogenation, hydration, methylation with oxylation, dehydrogenation with oxylation, and sulfation, have been observed in vivo. They were identified or tentatively identified by comparing their accurate mass data with prototypes and their metabolic pathways reported by the literature [39,40]. The metabolites for major phenolic compounds found in the urine and plasma samples were exhibited in Table 4.

Metabolites of phenolic compounds observed in vivo were mainly derived from the metabolism of liquiritigenin, isoliquiritigenin, and 6-gingerol, which were the most important aglycones from RGP and RZ in TSD. According to the MS data and the metabolic pathways reported in the literature, eleven related metabolites were identified in urine and plasma samples after the absorption of liquiritigenin and isoliquiritigenin. **M60** and **M61** showed $[M-H]^-$ ion at m/z 285.0765 ($C_{16}H_{13}O_5^+$), 30 Da (CH_2+O) heavier than parent compounds. In the MS/MS spectra, characteristic ions at m/z 270.05 $[M-H-CH_2]^-$ indicated the methyl substitution, and m/z 135.01 or 119.05 were used for the characterization of liquiritigenin or isoliquiritigenin derivatives. According to the polarity of liquiritigenin and isoliquiritigenin, **M60** and **M61** were confirmed as methyl-hydroxy liquiritigenin and methyl-hydroxy isoliquiritigenin. In vivo, liquiritigenin and isoliquiritigenin could be metabolized to a series of metabolites (**M41**, **M42**, **M50**, **M53**, **M54**, **M56**, **M57**, **M60**, **M61**, **M63**, and **M64**) by reaction of hydrogenation, dehydrogenation, hydroxylation, oxylation, hydration, methylation, and sulfation. In vivo, seven metabolites (**M43**, **M47**, **M48**, **M52**, **M55**, **M58**, and **M59**) of 6-gingerol were produced through the reaction of hydrogenation, methylation, hydration, hydroxylation, and dehydrogenation, with characteristic ions at m/z 163.08 or 137.06.

Table 4. Metabolites of phenolic compounds found in the urine and plasma samples.

ID	[M+H] ⁺ (m/z)	Formula	t _R (min)	Error (ppm)	ms/ms	Composition Change	Identification	Area	
								Urine	Plasma
M41.	259.09701	C ₁₅ H ₁₄ O ₄	17.57	2.53	153.0548, 135.0441, 107.0496	+H2	Hydrogenated liquiritigenin	++++	++
M42.	259.09689	C ₁₅ H ₁₄ O ₄	20.78	1.83	153.0549, 107.0497	+H2	Hydrogenated isoliquiritigenin	++++	+++
M43.	297.20602	C ₁₇ H ₂₈ O ₄	22.11	−0.23	177.0912, 163.0755, 137.0598, 131.0494	+H2	Hydrogenated 6-gingerol	++++	++
M44.	269.08170 ^{[M+H][−]}	C ₁₆ H ₁₄ O ₄	26.82	−0.03	254.0582, 153.0178, 135.0073, 91.0173	+H2	Hydrogenated formononetin	++++	++
M45.	367.11792 ^{[M+H][−]}	C ₂₁ H ₂₀ O ₆	29.54	−2.01	352.0936, 309.0400, 310.0434, 284.0325	+H2	Hydrogenated glycyrol	+++	+
M46.	355.15311	C ₂₁ H ₂₂ O ₅	30.71	−2.57	337.1065, 299.0912, 189.0911, 177.0546, 151.0393	+H2	Hydrogenated gancaonin M	++	
M47.	309.20578	C ₁₈ H ₂₈ O ₄	26.17	−0.70	163.0756, 137.0599, 131.0494	+CH2	Methyl 6-gingerol	++	
M48.	309.20572	C ₁₈ H ₂₈ O ₄	26.80	−0.92	179.0704, 150.068, 137.0598, 83.0864	+CH2	Methyl 6-gingerol	++	
M49.	285.07587	C ₁₆ H ₁₂ O ₅	18.49	0.51	270.0525, 253.0499, 299.0866, 225.0546, 123.0443	+O	Hydroxy formononetin	+++	
M50.	273.07593	C ₁₅ H ₁₂ O ₅	19.06	0.72	255.066, 179.0339, 153.0184, 147.0442, 123.044, 119.0496	+O	Hydroxy liquiritigenin/isoliquiritigenin	+++	++
M51.	369.13266	C ₂₁ H ₂₀ O ₆	29.18	−1.71	351.1222, 229.0860, 193.0497, 165.0548, 151.0389	+O	Hydroxy gancaonin M	+++	+
M52.	313.20038	C ₁₇ H ₂₈ O ₅	15.07	−0.96	203.1066, 163.0754, 137.0598	+H2O	Hydrated 6-gingerol	+++	
M53.	273.07629 ^{[M+H][−]}	C ₁₅ H ₁₄ O ₅	20.08	−1.36	255.0661, 167.0337, 109.0279	+H2O	Hydrated liquiritigenin	+++	
M54.	273.07660 ^{[M+H][−]}	C ₁₅ H ₁₄ O ₅	23.05	−0.68	255.0655, 151.0387, 135.0072, 109.0280	+H2O	Hydrated isoliquiritigenin	+++	
M55.	293.17447	C ₁₇ H ₂₄ O ₄	16.57	−0.91	163.0756, 137.0598, 99.0811	-H2	Dehydrogenated 6-gingerol	++	+
M56.	255.06552	C ₁₅ H ₁₀ O ₄	18.49	0.41	227.0703, 199.0756, 137.0234	-H2	Dehydrogenated liquiritigenin	+++	+
M57.	255.06550	C ₁₅ H ₁₀ O ₄	21.29	−0.16	227.0699, 199.0755, 137.0234	-H2	Dehydrogenated isoliquiritigenin	++++	+
M58.	307.15466 ^{[M+H][−]}	C ₁₇ H ₂₄ O ₅	26.17	−1.41	275.1288, 171.1014, 153.0907, 121.0280, 111.0799	-H2+O	Dehydrogenated-hydroxy 6-gingerol	++	
M59.	277.18039	C ₁₇ H ₂₄ O ₃	28.85	2.07	189.0914, 177.09123, 145.05493, 137.0597	-H2-O	Dehydrated 6-gingerol	++++	++
M60.	285.07648 ^{[M+H][−]}	C ₁₆ H ₁₄ O ₅	22.03	−0.35	270.0533, 153.0180, 149.0594, 135.0073, 134.0358, 91.0174	+CH2+O	Methyl-hydroxy liquiritigenin	+++	+
M61.	285.07645 ^{[M+H][−]}	C ₁₆ H ₁₄ O ₅	26.88	−1.06	270.0535, 153.0180, 149.0595, 135.0073, 91.0174	+CH2+O	Methyl-hydroxy isoliquiritigenin	++	
M62.	299.09170	C ₁₇ H ₁₄ O ₅	26.99	0.69	284.0680, 243.1061, 166.0268	+CH2+O	Methyl-hydroxy formononetin	+++	+
M63.	335.02261 ^{[M+H][−]}	C ₁₅ H ₁₂ O ₇ S	18.62	−1.33	255.0661, 199.0064, 135.0073, 119.0487	+SO3	Liquiritigenin sulfate	++++	+++
M64.	335.02271 ^{[M+H][−]}	C ₁₅ H ₁₂ O ₇ S	23.32	−0.94	255.0663, 199.0055, 135.0073, 119.0486	+SO3	Isoliquiritigenin sulfate	++++	++++
M65.	347.02263 ^{[M+H][−]}	C ₁₆ H ₁₂ O ₇ S	23.56	−1.41	267.0664, 252.0427	+SO3	Formononetin sulfate	++++	+++

Note: +, response area below 10⁶; ++, response area between 10⁶ and 10⁷; +++, response area between 10⁷ and 10⁸; +++++, response area above 10⁸.

3.4. Difference between Urine and Plasma Samples

Xenobiotics usually vary at trace levels and are interfered with endogenous components. Comparative analysis of metabolites between plasma and urine samples was carried out by the same LC-MS/MS method. Most prototype components and metabolites possessed suitable signal responses in urine samples, mainly as metabolites from phase I metabolism referring to dehydrogenation, demethylation, hydroxylation, deoxygenation, and deethylation. A few phase II metabolites were detected in the urine, including sulfate conjugates of liquiritigenin, isoliquiritigenin, and formononetin.

Metabolites of TSD detected in the plasma samples are fewer than those in the urine samples. As for plasma samples, 10 prototype components (eight phenolic compounds and two alkaloids) were detected and tentatively identified, most of which were flavonoid aglycones. Fifteen metabolites derived from neoline, talatizamine, karakoline songorine, and fuziline, as well as sixteen metabolites derived from liquiritigenin, isoliquiritigenin, formononetin, gancaonin M, and 6-gingerol, respectively, were found in plasma samples, which indicated there were fewer metabolites identified in plasma samples. These results are reasonable due to their relatively lower concentration and higher matrix interference in plasma than in urine samples.

In the present study, ADAs and their metabolites from RALP were mainly detected in rats after oral administration of TSD. DDAs are the most toxic but chemically unstable alkaloids in RALP, and the alkaloidal composition changed during decocting and decocting, with DDAs changing to MDAs, and both transformed further to ADAs while the toxicity gradually diminished. ADAs, such as fuziline and neoline, showed activity against pentobarbital sodium-induced cardiomyocyte damage by obviously recovering beating rhythm and increasing the cell viability [41]. Mesaconine and hypaconine showed strong cardiac actions on the isolated perfused bullfrog heart. Moreover, mesaconine has protective effects, including improved inotropic effect and left ventricular diastolic function, on myocardial ischemia-reperfusion injury in rats [42].

Metabolites of licorice flavonoids and 6-gingerol were also mainly detected. Liquiritigenin offers cytoprotective effects against various cardiac injuries, and it could protect against myocardial ischemic injury by antioxidation, antiapoptosis, counteraction mitochondrial dysfunction, and damping intracellular Ca^{2+} [43]. 6-Gingerol was identified as a novel angiotensin II type 1 receptor antagonist for cardiovascular disease by high-throughput screening, which partially clarified the mechanism of ginger regulating blood pressure and strengthening the heart [44]. 6-gingerol administration protected I/R-induced cardiomyocyte apoptosis via the JNK/NF- κ B pathway in the regulation of HMGB2 [45].

The results of the *in vivo* metabolite study of TSD in this study suggested that in the following pharmacokinetic, pharmacological, and efficacy studies, attention should be paid primarily to the ADAs alkaloids, licorice flavonoids, gingerol-6, and their metabolites

4. Conclusions

A total of 82 compounds, including 41 alkaloids, 35 phenolic compounds, and 6 saponins, were identified or tentatively characterized in TSD by UHPLC-Q-Exactive-MS/MS. Among them, 32 representative compounds with relatively high mass spectral peak areas and different core structures were selected as parent compound templates for further investigation of their metabolic profiles in rats. In total, 65 metabolites were screened out and tentatively characterized in rats' urine and plasma based on their MS characteristic fragmentation patterns and information. The main metabolic reactions involved hydrogenation, demethylation, hydroxylation, hydration, methylation, deoxygenation, and sulfation. This is a systematic study of *in vivo* metabolism of TSD, and it will be beneficial for further understanding of the pharmacological and pharmacokinetic study of TSD.

Supplementary Materials: The following supporting information can be downloaded at <https://www.mdpi.com/article/10.3390/metabo14060333/s1>, Figure S1: Workflow for the identification of prototype components, Figure S2: Workflow for the identification of metabolites, Figure S3: MS/MS spectra of major prototype compounds in the urine samples. Table S1: Compound information of in-house database, Table S2: Parameters of data processing by Compound Discoverer software.

Author Contributions: Conceptualization, G.D.; Methodology, W.X.; Formal analysis, X.Z., Y.Z. and M.P.; Data curation, X.Z. and Y.Z.; Writing—original draft, X.Z. and M.P.; Writing—review & editing, X.Z., W.X. and G.D.; Supervision, G.D.; Project administration, G.D.; Funding acquisition, G.D. All authors have read and agreed to the published version of the manuscript.

Funding: This research is supported by special funds for international cooperation from the Guangdong Provincial Hospital of Chinese Medicine (YN2024RD01) and the Scientific Research Project of Guangdong Provincial Bureau of Traditional Chinese Medicine (20231144).

Institutional Review Board Statement: All animal experiments were performed at the SPF animal laboratory [experimental animals license number SYXK (Guangdong, China) 2008–0094]. The Institutional Animal Ethics Committee of Guangdong Provincial Hospital of Chinese Medicine approved all experimental protocols (approval code: No. 2023131, approval date: 21 December 2023).

Informed Consent Statement: Not applicable.

Data Availability Statement: The data presented in this study are available on request from the corresponding author. The data are not publicly available due to confidentiality.

Conflicts of Interest: The authors declare no conflicts of interest.

References

1. He, L.Y.; Kang, Q.M.; Zhang, Y.; Chen, M.; Wang, Z.F.; Wu, Y.H.; Gao, H.T.; Zhong, Z.F.; Tan, W. Glycyrrhizae Radix et Rhizoma: The popular occurrence of herbal medicine applied in classical prescriptions. *Phytother. Res.* **2023**, *37*, 3135–3160. [[CrossRef](#)] [[PubMed](#)]
2. Lu, C.C.; Zhang, S.Y.; Lei, S.S.; Wang, D.N.; Peng, B.; Shi, R.P.; Chong, C.M.; Zhong, Z.F.; Wang, Y.T. A comprehensive review of the classical prescription Yiguan Jian: Phytochemistry, quality control, clinical applications, pharmacology, and safety profile. *J. Ethnopharmacol.* **2024**, *319*, 117230. [[CrossRef](#)] [[PubMed](#)]
3. Zhang, Q.; Han, X.-X.; Mao, C.-Q.; Xie, H.; Chen, L.-H.; Mao, J.; Lu, T.-L.; Yan, G.-J. Opportunities and challenges in development of compound preparations of traditional Chinese medicine: Problems and countermeasures in research of ancient classical prescriptions. *China J. Chin. Mater. Medica* **2019**, *44*, 4300–4308.
4. Chen, Z.K.; Wang, X.N.; Li, Y.Y.; Wang, Y.H.; Tang, K.L.; Wu, D.F.; Zhao, W.Y.; Ma, Y.M.; Liu, P.; Cao, Z.W. Comparative network pharmacology analysis of classical TCM prescriptions for chronic liver disease. *Front. Pharmacol.* **2019**, *10*, 1353. [[CrossRef](#)] [[PubMed](#)]
5. Chu, X.Y.; Wei, X.H.; Wu, X.F.; Chen, J.; Xia, H.; Xia, G.Y.; Lin, S.; Shang, H.C. Pharmacological research progress of five classical prescriptions in treatment of chronic heart failure. *China J. Chin. Mater. Medica* **2023**, *48*, 6324–6333.
6. Zhou, Q.; Meng, P.; Zhang, Y.; Chen, P.; Wang, H.B.; Tan, G.G. The compatibility effects of sini decoction against doxorubicin-induced heart failure in rats revealed by mass spectrometry-based serum metabolite profiling and computational analysis. *J. Ethnopharmacol.* **2020**, *252*, 112618. [[CrossRef](#)] [[PubMed](#)]
7. Chen, Q.; Xiao, S.; Li, Z.H.; Ai, N.; Fan, X.H. Chemical and Metabolic Profiling of Si-Ni Decoction Analogous Formulae by High performance Liquid Chromatography-Mass Spectrometry. *Sci. Rep.* **2015**, *5*, 11638. [[CrossRef](#)]
8. Chen, S.; Wu, S.; Li, W.H.; Chen, X.F.; Dong, X.; Tan, G.G.; Zhang, H.; Hong, Z.Y.; Zhu, Z.Y.; Chai, Y.F. Investigation of the therapeutic effectiveness of active components in Sini decoction by a comprehensive GC/LC-MS based metabolomics and network pharmacology approaches. *Mol. Biosyst.* **2014**, *10*, 3310–3321. [[CrossRef](#)] [[PubMed](#)]
9. Tan, G.G.; Wang, X.; Liu, K.; Dong, X.; Liao, W.T.; Wu, H. Correlation of drug-induced and drug-related ultra-high performance liquid chromatography-mass spectrometry serum metabolomic profiles yields discovery of effective constituents of Sini decoction against myocardial ischemia in rats. *Food Funct.* **2018**, *9*, 5528–5535. [[CrossRef](#)]
10. Hu, Q.; Chen, M.; Yan, M.M.; Wang, P.L.; Lei, H.M.; Xue, H.Y.; Ma, Q. Comprehensive analysis of Sini decoction and investigation of acid-base self-assembled complexes using cold spray ionization mass spectrometry. *Microchem. J.* **2020**, *173*, 107008. [[CrossRef](#)]
11. Zhang, H.; Liu, M.; Zhang, W.; Chen, J.; Zhu, Z.Y.; Cao, H.; Chai, Y.F. Comparative pharmacokinetics of three monoester-diterpenoid alkaloids after oral administration of *Acontium carmichaeli* extract and its compatibility with other herbal medicines in Sini Decoction to rats. *Biomed. Chromatogr.* **2015**, *29*, 1076–1083. [[CrossRef](#)]
12. Zhou, Q.; Meng, P.; Wang, H.B.; Dong, X.; Tan, G.G. Pharmacokinetics of monoester-diterpenoid alkaloids in myocardial infarction and normal rats after oral administration of Sini decoction by microdialysis combined with liquid chromatography-tandem mass spectrometry. *Biomed. Chromatogr.* **2019**, *33*, e4406. [[CrossRef](#)] [[PubMed](#)]

13. Sun, S.; Chen, Q.S.; Ge, J.Y.; Liu, X.; Wang, X.X.; Zhan, Q.; Zhang, H.; Zhang, G.Q. Pharmacokinetic interaction of aconitine, liquiritin and 6-gingerol in a traditional Chinese herbal formula. *Sini Decoction* **2018**, *48*, 45–52. [[CrossRef](#)]
14. Zhou, J.; Ma, X.Q.; Shi, M.; Chen, C.W.; Sun, Y.; Li, J.J.; Xiong, Y.X.; Chen, J.J.; Li, F.Z. Serum metabolomics analysis reveals that obvious cardioprotective effects of low dose Sini decoction against isoproterenol-induced myocardial injury in rats. *Phytomedicine* **2017**, *31*, 18–31. [[CrossRef](#)] [[PubMed](#)]
15. Bai, S.S.; Luo, D.W.; Zhong, G.Y.; Yang, S.L.; Ouyang, H.; Rao, X.Y.; Feng, Y.L. Exploration of plant metabolomics variation and absorption characteristics of water-extracted *Rheum tanguticum* and ethanol-extracted *Rheum tanguticum* by UHPLC-Q-TOF-MS/MS. *Phytochem. Anal.* **2024**, *35*, 288–307. [[CrossRef](#)]
16. Ye, L.H.; He, X.X.; Yan, M.Z.; Chang, Q. Identification of in vivo components in rats after oral administration of lotus leaf flavonoids using ultra fast liquid chromatography with tandem mass spectrometry. *Anal. Methods* **2014**, *6*, 6088–6094. [[CrossRef](#)]
17. Tao, J.H.; Zhao, M.; Jiang, S.; Zhang, W.; Xu, B.H.; Duan, J.A. UPLC-Q-TOF/MS-based metabolic profiling comparison of four major bioactive components in normal and CKD rat plasma, urine and feces following oral administration of *Cornus officinalis* Sieb and *Rehmannia glutinosa* Libosch herb couple extract. *J. Pharm. Biomed. Anal.* **2018**, *161*, 254–261. [[CrossRef](#)]
18. Deng, F.; Li, X.M.; Gong, Q.Q.; Zheng, Z.X.; Zeng, L.; Zhang, M.J.; Duan, T.Y.; Liu, X.; Zhang, M.Z.; Guo, D.L. Identification of in vivo metabolites of *Citri Sarcodactylis Fructus* by UHPLC-Q/Orbitrap HRMS. *Phytochem. Anal.* **2023**, *34*, 938–949. [[CrossRef](#)] [[PubMed](#)]
19. Zhang, X.J.; Liu, S.; Xing, J.P.; Pi, Z.F.; Liu, Z.Q.; Song, F.R. Systematic study on metabolism and activity evaluation of Radix *Scutellaria* extract in rat plasma using UHPLC with quadrupole time-of-flight mass spectrometry and microdialysis intensity-fading mass spectrometry. *J. Sep. Sci.* **2018**, *41*, 1704–1710. [[CrossRef](#)]
20. Huang, J.; Zhang, J.P.; Bai, J.Q.; Wei, M.J.; Zhang, J.; Huang, Z.H.; Qu, G.H.; Xu, W.; Qiu, X.H. Chemical profiles and metabolite study of raw and processed *Polygoni Multiflori Radix* in rats by UPLC-LTQ-Orbitrap MSⁿ spectrometry. *Chin. J. Nat. Med.* **2018**, *16*, 375–400.
21. Su, C.Y.; Wang, J.H.; Chang, T.Y.; Shih, C.L. Mass defect filter technique combined with stable isotope tracing for drug metabolite identification using high-resolution mass spectrometry. *Anal. Chim. Acta* **2022**, *1208*, 339814. [[CrossRef](#)] [[PubMed](#)]
22. Zhou, X.H.; Chen, X.; Yin, X.M.; Wang, M.Y.; Zhao, J.J.; Ren, Y. A strategy integrating parent ions list-modified mass defect filtering-diagnostic product ions for rapid screening and systematic characterization of flavonoids in *Scutellaria barbata* using hybrid quadrupole-orbitrap high-resolution mass spectrometry. *J. Chromatogr. A* **2022**, *1674*, 463149. [[CrossRef](#)]
23. Wang, B.L.; Lu, Y.M.; Hu, X.L.; Feng, J.H.; Shen, W.; Wang, R.; Wang, H. Systematic Strategy for Metabolites of Amentoflavone In Vivo and In Vitro Based on UHPLC-Q-TOF-MS/MS Analysis. *J. Agric. Food Chem.* **2020**, *68*, 14808–14823. [[CrossRef](#)] [[PubMed](#)]
24. Xu, W.; Zhang, J.; Zhu, D.Y.; Huang, J.; Huang, Z.H.; Bai, J.Q.; Qiu, X.H. Rapid separation and characterization of diterpenoid alkaloids in processed roots of *Aconitum carmichaeli* using ultra high performance liquid chromatography coupled with hybrid linear ion trap-Orbitrap tandem mass spectrometry. *J. Sep. Sci.* **2014**, *37*, 2864–2873. [[CrossRef](#)] [[PubMed](#)]
25. Cai, X.F.; XU, Y.; Liu, H.P.; Shang, Q.; Qiu, J.Q.; Xu, W. Chemical analysis of classical prescription Qianghuo Shengshi standard decoction by UHPLC-Q Exactive Orbitrap MS. *China J. Chin. Mater. Medica* **2022**, *47*, 343–357.
26. Lu, F.Y.; Cai, H.; Li, S.M.; Xie, W.; Sun, R.J. The Chemical Signatures of Water Extract of *Zingiber officinale* Rosc. *Molecules* **2022**, *27*, 7818. [[CrossRef](#)] [[PubMed](#)]
27. Meng, X.Y.; Li, H.L.; Song, F.R.; Liu, C.M.; Liu, Z.Q.; Liu, S.Y. Studies on Triterpenoids and Flavones in *Glycyrrhiza uralensis* Fisch by HPLC-ESI-MSⁿ and FT-ICR-MSⁿ. *Chin. J. Chem.* **2009**, *27*, 299–305. [[CrossRef](#)]
28. Avula, B.; Bae, J.Y.; Chittiboyina, A.G.; Wang, Y.H.; Wang, M.; Zhao, J.P.; Ali, Z.; Brinckmann, J.A.; Li, J.; Wu, C. Chemometric analysis and chemical characterization for the botanical identification of *Glycyrrhiza* species (*G. glabra*, *G. uralensis*, *G. inflata*, *G. echinata* and *G. lepidota*) using liquid chromatography-quadrupole time of flight mass spectrometry (LC-QToF) Bharathi. *J. Food Compos. Anal.* **2022**, *112*, 104679.
29. Zhang, J.; Huang, Z.H.; Qiu, X.H.; Yang, Y.M.; Zhu, D.Y.; Xu, W. Neutral fragment filtering for rapid identification of new diester-diterpenoid alkaloids in roots of *Aconitum carmichaeli* by ultra-high-pressure liquid chromatography coupled with linear ion trap-Orbitrap mass spectrometry. *PLoS ONE* **2012**, *7*, e52352. [[CrossRef](#)]
30. He, G.N.; Wang, X.X.; Liu, W.R.; Li, Y.L.; Shao, Y.M.; Liu, W.D.; Liang, X.D.; Bao, X. Chemical constituents, pharmacological effects, toxicology, processing and compatibility of Fuzi (lateral root of *Aconitum carmichaelii* Debx): A review. *J. Ethnopharmacol.* **2023**, *307*, 116160. [[CrossRef](#)]
31. Chen, X.; Tan, P.; He, R.; Liu, Y.G. Study on the fragmentation pathway of the aconitine-type alkaloids under electrospray ionization tandem mass spectrometry utilizing quantum chemistry. *J. Pharm. Innov.* **2013**, *8*, 83–89. [[CrossRef](#)]
32. Hu, R.; Zhao, J.; Qi, L.W.; Li, P.; Jing, S.L.; Li, H.J. Structural characterization and identification of C19- and C20-diterpenoid alkaloids in roots of *Aconitum carmichaeli* by rapid-resolution liquid chromatography coupled with time-of-flight mass spectrometry. *Rapid Commun. Mass Spectrom.* **2009**, *23*, 1619–1635. [[CrossRef](#)] [[PubMed](#)]
33. Lv, L.S.; Soroka, D.; Chen, X.X.; Leung, T.C.; Sang, S.M. 6-Gingerdiols as the major metabolites of 6-gingerol in cancer cells and in mice and their cytotoxic effects on human cancer cells. *Agric Food Chem.* **2012**, *60*, 11372–11377. [[CrossRef](#)] [[PubMed](#)]
34. Pham, H.N.; Tran, C.A.; Trinh, T.D.; Thi, N.L.N.; Phan, H.N.; Le, V.N.; Le, N.H.; Phung, V. UHPLC-Q-TOF-MS/MS Dereplication to identify chemical constituents of *Hedera helix* leaves in Vietnam. *J. Anal. Methods Chem.* **2022**, *2022*, 1167265. [[CrossRef](#)] [[PubMed](#)]

35. Savarino, P.; Demeyer, M.; Decroo, C.; Colson, E.; Gerbaux, P. Mass spectrometry analysis of saponins. *Mass Spectrom. Rev.* **2023**, *42*, 954–983. [[CrossRef](#)] [[PubMed](#)]
36. Zhang, Z.; Jiang, M.Y.; Wei, X.Y.; Shi, J.F.; Geng, Z.; Yang, S.S.; Fu, C.M.; Guo, L. Rapid discovery of chemical constituents and absorbed components in rat serum after oral administration of Fuzi-Lizhong pill based on high-throughput HPLC-Q-TOF/MS analysis. *Chin. Med.* **2019**, *14*, 6. [[CrossRef](#)] [[PubMed](#)]
37. Cao, Y.; Chen, X.F.; Lu, D.Y.; Dong, X.; Zhang, G.Q.; Chai, Y.F. Using cell membrane chromatography and HPLC-TOF/MS method for in vivo study of active components from roots of *Aconitum carmichaeli*. *J. Pharm. Anal.* **2011**, *1*, 125–134. [[PubMed](#)]
38. Zhang, M.; Peng, C.; Li, X.B. In vivo and in vitro metabolites from the main diester and monoester diterpenoid alkaloids in a traditional Chinese herb, the *Aconitum* species. *Evid. Based Complement. Altern. Med.* **2015**, *2015*, 252434.
39. Zhang, L.; Wang, C.X.; Wu, J.; Wang, T.Y.; Zhong, Q.Q.; Du, Y.; Ji, S.; Wang, L.; Guo, M.Z.; Xu, S.Q. Metabolic profiling of mice plasma, bile, urine and feces after oral administration of two licorice flavonones. *J. Ethnopharmacol.* **2020**, *257*, 112892. [[CrossRef](#)]
40. Li, Y.Y.; Yang, L.; Chai, X.; Yang, J.J.; Wang, Y.F.; Zhu, Y. Four major urinary metabolites of liquiritigenin in rats and their anti-platelet aggregation activity. *Chem. Nat. Compd.* **2018**, *54*, 443–446. [[CrossRef](#)]
41. Xiong, L.; Peng, C.; Xie, X.F.; Guo, L.; He, C.J.; Geng, Z.; Wan, F.; Dai, O.; Zhou, Q.M. Alkaloids Isolated from the Lateral Root of *Aconitum carmichaelii*. *Molecules* **2012**, *17*, 9939–9946. [[CrossRef](#)] [[PubMed](#)]
42. Liu, X.X.; Jian, X.X.; Cai, X.F.; Chao, R.B.; Chen, Q.H.; Chen, D.L.; Wang, X.L.; Wang, F.P. Cardioactive C₁₉-diterpenoid alkaloids from the lateral roots of *Aconitum carmichaeli* “Fu Zi”. *Chem. Pharm. Bull.* **2012**, *60*, 144–149. [[CrossRef](#)] [[PubMed](#)]
43. Zhang, M.Q.; Qi, J.Y.; He, Q.Q.; Ma, D.L.; Li, J.; Chu, X.; Zuo, S.J.; Zhang, Y.X.; Li, L.; Chu, L. Liquiritigenin protects against myocardial ischemic by inhibiting oxidative stress, apoptosis, and L-type Ca²⁺ channels. *Phytother. Res.* **2022**, *36*, 3619–3631. [[CrossRef](#)] [[PubMed](#)]
44. Liu, Q.; Liu, J.J.; Guo, H.L.; Sun, S.N.; Wang, S.F.; Zhang, Y.L.; Li, S.Y.; Qiao, Y.J. [6]-Gingerol: A Novel AT₁ Antagonist for the Treatment of Cardiovascular Disease. *Planta Medica* **2013**, *79*, 322–326. [[CrossRef](#)]
45. Zhang, W.Y.; Liu, X.Y.; Jiang, Y.P.; Wang, N.N.; Li, F.; Xin, H.L. 6-Gingerol attenuates ischemia-reperfusion-induced cell apoptosis in human AC16 cardiomyocytes through HMGB2-JNK1/2-NF-κB pathway. *Evid. Based Complement. Altern.* **2019**, *2019*, 8798653. [[CrossRef](#)] [[PubMed](#)]

Disclaimer/Publisher’s Note: The statements, opinions and data contained in all publications are solely those of the individual author(s) and contributor(s) and not of MDPI and/or the editor(s). MDPI and/or the editor(s) disclaim responsibility for any injury to people or property resulting from any ideas, methods, instructions or products referred to in the content.